Local Sensitivities of the Gulf Stream Separation[a]

JOSEPH SCHOONOVER

Center for Nonlinear Studies, Los Alamos National Laboratory, Los Alamos, New Mexico

WILLIAM K. DEWAR, NICOLAS WIENDERS, AND BRUNO DEREMBLE

Department of Earth, Ocean, and Atmospheric Sciences, Florida State University, Tallahassee, Florida

(Manuscript received 24 August 2016, in final form 22 November 2016)

ABSTRACT

Robust and accurate Gulf Stream separation remains an unsolved problem in general circulation modeling whose resolution will positively impact the ocean and climate modeling communities. Oceanographic literature does not face a shortage of plausible hypotheses that attempt to explain the dynamics of the Gulf Stream separation, yet a single theory that the community agrees on is missing. In this paper, the authors investigate the impact of the deep western boundary current (DWBC), coastline curvature, and continental shelf steepening on the Gulf Stream separation within regional configurations of the Massachusetts Institute of Technology General Circulation Model. Artificial modifications to the regional bathymetry are introduced to investigate the sensitivity of the separation to each of these factors. Metrics for subsurface separation detection confirm the direct link between flow separation and the surface expression of the Gulf Stream in the Mid-Atlantic Bight. It is shown that the Gulf Stream separation and mean surface position are most sensitive to the continental slope steepening, consistent with a theory proposed by Melvin Stern in 1998. In contrast, the Gulf Stream separation exhibits minimal sensitivity to the presence of the DWBC and coastline curvature. The implications of these results to the development of a "separation recipe" for ocean modeling are discussed. This study concludes adequate topographic resolution is a necessary, but not sufficient, condition for proper Gulf Stream separation.

1. Introduction

a. *Gulf Stream separation in numerical models*

Coarse-resolution simulations of the general circulation notoriously produce poorly behaved western boundary currents. In the case of the coarsely resolved North Atlantic, the Gulf Stream is often found separating far north of its observed separation latitude. The surface signature of the Gulf Stream consists of warm, fast-moving [$O(1)\,\mathrm{m\,s^{-1}}$] waters that dominate the heat exchange with the atmosphere. The northward bias of the modeled Gulf Stream in the Mid-Atlantic Bight has been hypothesized to be due to a number of processes related to its separation and interior pathway. In coupled climate simulations, such a bias leads to a systematic error that can erode the fidelity of climate predictions (Saba et al. 2016) and has also been shown to have an impact on coastal sea level rise predictions (Ezer et al. 2013). The focus of this paper is on the impacts local processes have on the Gulf Stream pathway as it travels between the South Atlantic Bight and the Mid-Atlantic Bight and separates from the continental slope.

Increased model resolution that resolves the first baroclinic deformation radius can improve western boundary current behavior, though the Gulf Stream separation has been shown to be sensitive to subgrid-scale parameterizations (Bryan et al. 2007) and vertical grid type (Ezer 2016). Schoonover et al. (2016) found that a northward bias in the Gulf Stream separation is linked to a more viscous vorticity balance on scales less than 100 km compared to models with a more accurate separation. The reason for such a sensitivity and correlation between increased viscosity and northward separation is unclear. Hurlburt and Hogan (2008) suggest that increased viscosity can damp offshore (OS) eddy activity, thereby weakening deep recirculations that would normally guide the Gulf Stream through the Mid-Atlantic Bight. The need of ocean models to maintain a robust recirculation gyre in

[a] Los Alamos National Laboratory Publication Number LA-UR-16-25889.

Corresponding author e-mail: Joseph Schoonover, jschoonover@lanl.gov

DOI: 10.1175/JPO-D-16-0195.1

the Mid-Atlantic Bight to achieve realistic offshore Gulf Stream pathway (postseparation) has also been demonstrated by Ezer and Mellor (1992). Bryan et al. (2007) suggest that the higher viscosity creates a weaker deep western boundary current (DWBC) that is incapable of keeping the separation point at Cape Hatteras (CH), similar to a mechanism described by Tansley and Marshall (2000). Additionally, a weak DWBC has previously been shown to result in a weak northern recirculation gyre, which permits a northward migration of the separated Gulf Stream (Zhang and Vallis 2007). Processes that involve direct interactions of the Gulf Stream with features such as topography or the deep western boundary current are considered local processes and are the primary focus of this study. Although, nonlocal processes may influence the Gulf Stream separation latitude and separated pathway, uncovering the local sensitivities will guide the formulation of a theory for separation from the continental slope. Such a theory should then allow for extension to incorporate nonlocal effects.

The community's modeling experience provides details that a separation theory should explain. The resolution dependence of the separation indicates that the separation relies on length scales smaller than the deformation radius in the flow, forcing, or bathymetry. The correlation of northward separation to increased Laplacian or biharmonic diffusion and mixing (subgrid-scale parameterization) is consistent with this length-scale dependence. Increasing, for example, the momentum diffusion effectively reduces the amount of energy present in smaller scales of an eddy-resolving simulation. It is possible then that the energy damping of the smaller scales is disrupting the separation process. A theory for the Gulf Stream separation should be able to explain why such resolution/length-scale dependencies exist in addition to why Cape Hatteras is such a unique place for the Gulf Stream to head offshore.

b. *Literature*

The Gulf Stream separation has seen much attention in the literature (Charney 1955; Parsons 1969; Sarkisyan and Ivanov 1971; Holland 1972; Thompson and Schmitz 1989; Stern and Whitehead 1990; Haidvogel et al. 1992; Ezer and Mellor 1992; Agra and Nof 1993; Dengg 1993; Pickart and Smethie 1993; Pickart 1994; Spall 1996; Ozgokmen et al. 1997; Stern 1998; Tansley and Marshall 2000; Munday and Marshall 2005; Zhang and Vallis 2007; Hurlburt and Hogan 2008; Hurlburt et al. 2011; Ezer 2016). Hurlburt et al. (2011) and Ezer (2016) outline the history of the Gulf Stream separation modeling; a thorough review up to 2008 appears in Chassignet and Marshall (2008). This considerable amount of attention has led to the development of many plausible hypotheses to explain the separation, yet a clear preference for any one of the mechanisms has not emerged, and it is likely that separation is affected by a combination of factors such as model configuration, parameterizations, and forcing used. An interesting reoccurring theme on the Gulf Stream separation is the stability of the separation latitude on seasonal and interannual time scales that was first reported by Auer (1987). Even in the extreme deflections in the offshore Gulf Stream pathway reported in Gawarkiewicz et al. (2012), the inshore position near Cape Hatteras remained fixed [see Figs. 4 and 5 of Gawarkiewicz et al. (2012)]. Tansley and Marshall (2000) point out that the stationarity of the Gulf Stream separation is particular to the North Atlantic, citing a comparison to the Brazil and Malvinas Currents made by Olson et al. (1988). The persistence of the Gulf Stream separation latitude suggests that local processes particular to the Mid- and South Atlantic Bight are in control of the Gulf Stream separation and that the separation latitude is not primarily controlled by seasonally varying wind stress and heat flux patterns.

1) Coastline curvature

Even while focusing on the unique features of the Gulf Stream system, it has been a difficult task to determine the process that dominantly controls the separation process. Many of the modeling studies focused on rather idealized representations of the Gulf Stream system that accentuated one process while neglecting others. For example, Dengg (1993) modeled the North Atlantic as a flat-bottom barotropic fluid with vertical sidewalls. A sharp turn was introduced in the coastline in order to isolate the effects of coastline curvature on the separation. Motivated by the fact the real ocean has variable bathymetry and is stratified, Ozgokmen et al. (1997) added to Dengg's model by treating the ocean as a two-layer system with topography confined to the lowest layer. In general, the two studies revealed similar results: in order to achieve proper separation in their models, a viscous sublayer within the inertial Gulf Stream is required to generate sufficient cyclonic vorticity in order to maintain a recirculation past the turn in the coastline. Ozgokmen et al. (1997) refined Dengg's separation theory by pointing out that sufficient inertia is required in order for the Gulf Stream to cross the background potential vorticity contours imposed by the shelf bathymetry.

Marshall and Tansley (2001) illustrated that the downstream increase in the Coriolis parameter, the beta effect, can inhibit separation past a coastal promontory. This conclusion was reached based on three arguments: 1) Classic boundary layer theory indicates that flow separation is coincident with an adverse pressure gradient (Batchelor 2000). 2) For an inviscid and hydrostatic fluid, flow deceleration is equivalent to the presence of an adverse pressure gradient along density surfaces. 3) Steady-state inviscid energy and vorticity balances link the beta effect to flow acceleration and a cyclonic turn in the coastline to flow deceleration. Since it is assumed that flow deceleration is coincident with flow separation, the coastline curvature must be sufficient to overcome the acceleration caused by the beta effect. The theory presented by Marshall and Tansley (2001) provided a condition for separation:

$$R < (U/\beta^*)^{1/2}, \tag{1}$$

where R is the radius of curvature of the coastline, U is the flow speed, and β^* is the gradient in the Coriolis parameter in the direction of the flow. Then, four years later, Munday and Marshall (2005) confirmed the separation condition within idealized flat-bottomed, shallow-water simulations. These models of the Gulf Stream system, however, neglected the effects of the deep western boundary current and a more realistic continental slope that directly interacts with both the Gulf Stream and the deep flow.

2) Deep western boundary current

Tansley and Marshall (2000) investigated the impacts of the continental shelf geometry at Cape Hatteras and the deep western boundary current in an idealized modeling configuration while neglecting the effects of coastline curvature. The processes were modeled using the two-layer geostrophic vorticity equations. As in Ozgokmen et al. (1997), the variable bathymetry was confined to the deep layer. Tansley and Marshall (2000) pointed out that the shelf widening that occurs south of Cape Hatteras controls the location at which the Gulf Stream must cross over the DWBC. They showed that localized downwelling occurs at the crossover and is linked to the DWBC descending down the continental slope in an effort to conserve its potential vorticity. This process is identical to the potential vorticity conservation arguments of Hogg and Stommel (1985) and is consistent with observations (Pickart and Smethie 1993) and other idealized model solutions (Spall 1996) of the crossover. The observed downwelling at the separation was linked to vortex tube stretching of the upper-layer flow that is consistent with flow deceleration and, again by Bernoulli's theorem, an adverse pressure gradient. The separation latitude was shown to be correlated with the location of the continental shelf widening and the strength of the prescribed DWBC. When the shelf widening was introduced, the separation was displaced southward but was found to exhibit substantial variability. The separation latitude transitioned between two preferred locations with a time scale on the order of hundreds of days. Increasing the DWBC transport led to more frequent occupation of the more southerly separation position, but the variability present in the model is inconsistent with the observed Gulf Stream.

Multiyear observations of the deep flow just offshore of Cape Hatteras suggest that the DWBC plays a more passive role in the separation process at the crossover (Pickart 1994). On long time scales, greater than 1 yr, the variations in the orientation and the transport of the DWBC lag variations in the Gulf Stream orientation and transport by (roughly) 1 month. Pickart (1994) argued that fluctuations in the Gulf Stream on these time scales are therefore not caused by the DWBC, but instead the DWBC is directly influenced by the Gulf Stream. Pickart (1995) illustrated that the variability in the deep flow is linked to topographic Rossby waves with a 40-day period generated by meanders in the Gulf Stream path far from the separation. Pickart found that the mean orientation of the Gulf Stream and the local topographic wave ray paths are in alignment. It is suggested that this configuration of the mean flow is stable in that the energetic topographic waves act to force the mean Gulf Stream pathway to remain in its mean position through the counterpropagation of wave energy. "Thus while the DWBC does not seem to alter the Gulf Stream separation, it is intriguing to speculate that the strong topographic waves do. Such a notion deserves further attention" (Pickart 1994, p. 163).

3) Continental shelf geometry

Interestingly, Stern (1998) provided the only separation theory that incorporates the interaction of the Gulf Stream with locally generated continental shelf waves. Additionally, it was the first analytical model that attempted to incorporate variable bathymetry that extended through both layers of a 1.5-layer model. The Stern model idealized the Gulf Stream as a barotropic current with a constant vorticity that flows partially over a continental slope and partially over a resting deep layer (see Fig. 1). The fluid in the lower layer offshore is assumed to be motionless. A small steepening in the continental slope is introduced, similar to the observed bathymetry between the Charleston Bump (CB) and Cape Hatteras (see Fig. 2a). The steepening of the continental shelf instigates the growth of shelf waves that consequently interact with the upstream flow; such interactions had been documented previously in the barotropic modeling study of Hughes (1986). Stern demonstrated that when the upstream flow matches the speed of the barotropic shelf waves that are generated

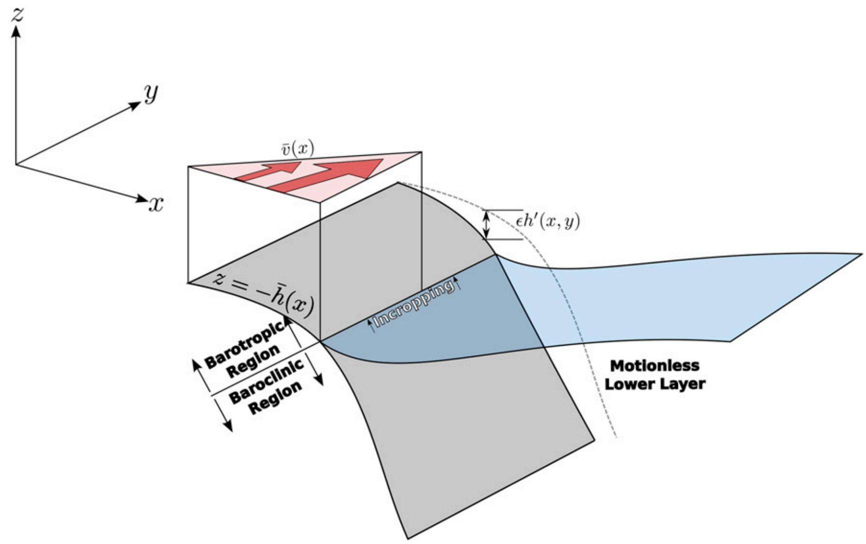

FIG. 1. A recreation of the schematic that appears in Fig. 2 of Stern (1998) and highlights the essential ingredients of the model for separation. A current with cyclonic shear flows over a continental slope, which steepens in the downstream direction. At the incropping, a boundary condition is enforced that ensures kinetic energy and fluid thickness conservation as fluid parcels exit the barotropic region.

by the steepening, a resonant interaction occurs between the prescribed flow and the shelf waves that lead to flow separation. A distinction is made between flows that are ''subcritical,'' slower than the shelf waves, and ''supercritical.'' Namely, subcritical flows over a steepening shelf result in the flow remaining attached, while critical and supercritical flows are able to separate.

c. Approach

Although the idealized models demonstrate how individual processes may lead to separation, there is no direct way to comment on the relative importance of each. In this paper, we investigate the impact of the DWBC, coastline curvature, and continental slope geometry within a realistic regional simulation of the Gulf Stream. Separate experiments are conducted in which modifications to the bathymetry are made in order to steer the DWBC away from the usual crossover, remove the turn in the coastline at Cape Hatteras, and remove the continental slope steepening (a necessary ingredient of the Stern model). Given that the scope of this paper is limited to a select set of local processes, we do not systematically modify boundary conditions or atmospheric forcing, preferring instead to use realistic HYCOM and basic ECMWF fields. Of course, relative to the latter, our heat and water fluxes are computed by supplying the needed atmospheric fields into our atmospheric boundary layer package, the Cheap Atmospheric Mixed Layer (CheapAML), the details of which appear in Deremble et al. (2013). In the experiments presented, it will be shown that the Gulf Stream separation is most sensitive to changes in the continental shelf geometry in a manner consistent with the theory of Stern (1998). The separation latitude shows a remarkable insensitivity to the presence of the DWBC at the usual crossover, consistent with the hypothesis suggested by Pickart (1994), and the coastline curvature. The paper proceeds by introducing the model configuration and the techniques used for describing and detecting the separation in sections 2a and 2b, respectively. The results of the sensitivity experiments are presented in section 3 followed by a discussion in section 4.

2. Methods

a. Model configuration

To isolate our focus on the separation of the Gulf Stream, a simulation is conducted using the Massachusetts Institute of Technology General Circulation Model (MITgcm; Marshall et al. 1997). The domain is confined to the region bounded by latitudes (22.6°, 42°N) and longitudes (278°, 298.7°E) and uses a nominal resolution of 10 km. The construction of the vertical grid is motivated by the desire to have increased resolution at the depths at which the Gulf Stream interacts with the continental shelf, between 500 and 1000 m. The vertical grid spacing is 32 m near the surface, decreases to 20 m between 500- and 1000-m depth, and gradually increases to 215 m at the maximum depth of 5600 m. The control

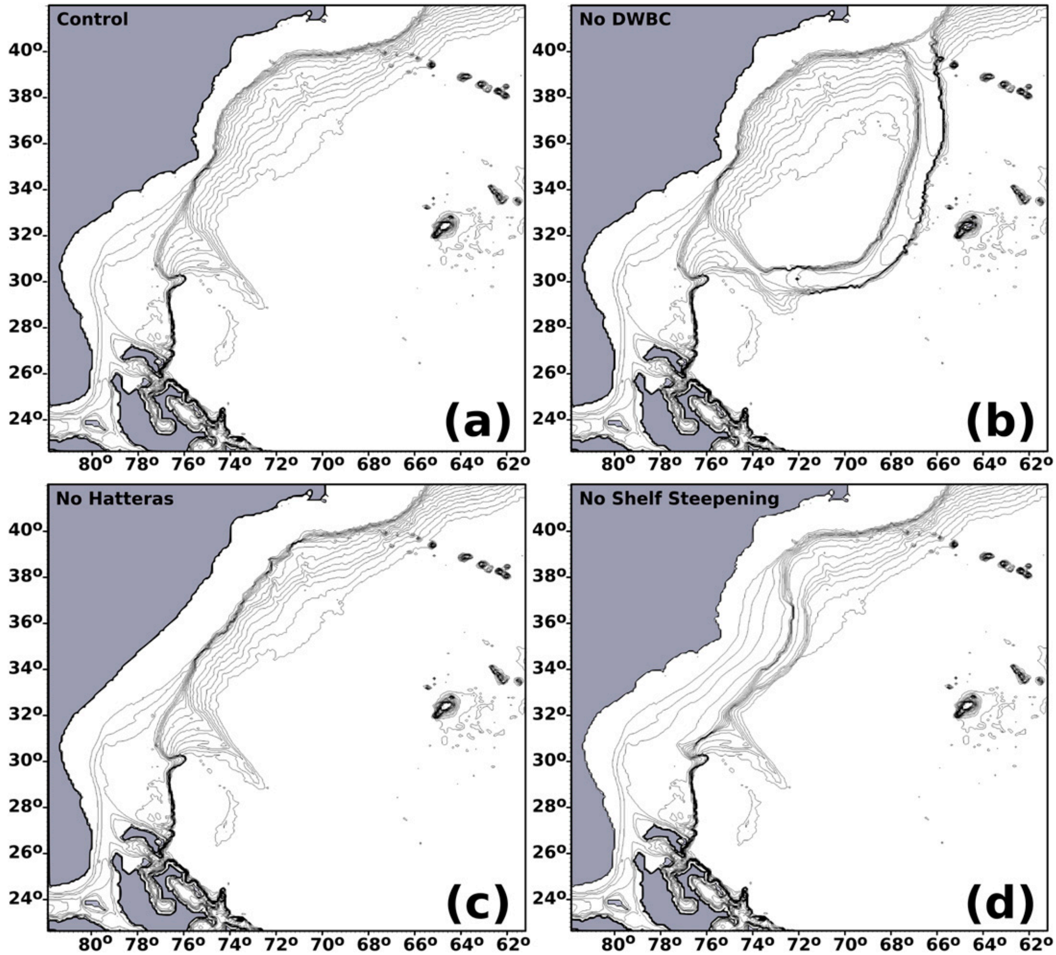

FIG. 2. (a) The bathymetry for the control simulation, derived from the ETOPO1 dataset of Amante and Eakins (2009). (b) The bathymetry for the terraforming experiment where the DWBC is prevented from interacting with the Gulf Stream near Cape Hatteras. An artificial ridge is introduces that intercepts the DWBC near its inflow and guides it southward toward the Blake Ridge. (c) The bathymetry for the No Hatteras experiment, where the turn in the coastline and continental slope is removed. (d) The bathymetry for the Add Slope experiment, where the continental slope is widened from the Charleston Bump northward, past Cape Hatteras, and the steepening zone is effectively placed around 39°N. All isobaths are shown in increments of 250 m.

simulation uses bathymetry derived from the ETOPO1, the 1-min resolution dataset of Amante and Eakins (2009). Before interpolating onto the model grid, the bathymetry is smoothed using a Gaussian filter with a half-width of 10 km (see Fig. 2a for the bathymetry from the control simulation) in order to reduce the impact of grid-scale variations in the topography. Partial bottom cells are used to improve the accuracy of the bottom representation (Adcroft et al. 1997), with a minimum cell fraction of 40%.

Boundary and initial conditions are taken from the HYCOM + NCODA global assimilative model solutions (experiment GLBa0.08) with nominal resolution of 10 km. The HYCOM ocean state is climatologically averaged over the HYCOM model years 2004–08 and detrended to provide a single year of climatological boundary conditions that are repeated. A sponge layer that is 50 km thick (five grid points) is used on all of the model boundaries to relax the solution to the HYCOM boundary conditions on a time scale of 2 days at the innermost grid cells and 1 day on the outermost grid cells. The relaxation vanishes one grid point beyond the sponge layer. Although this configuration results in a jump discontinuity in the relaxation conditions, no adverse effects were apparent upon inspection.

Momentum, heat, and moisture fluxes are calculated using a boundary layer model, CheapAML (Deremble et al. 2013), which takes into account the surface ocean state in the flux calculations. Atmospheric conditions, the 10-m wind velocity, surface solar radiation, specific humidity, and air temperature are derived from the ERA-Interim reanalysis dataset. As with the boundary conditions, years 2000–04 are climatologically averaged and detrended to yield a single year of atmospheric conditions.

Lateral diffusive fluxes of momentum, heat, and salt are calculated using biharmonic diffusion with a diffusion coefficient of $10^{10}\,\mathrm{m^4\,s^{-1}}$. Vertical diffusion of momentum, heat, and salt is calculated using an explicit vertical Laplacian diffusion with a coefficient of $10^{-5}\,\mathrm{m^2\,s^{-1}}$. Additional vertical mixing is calculated implicitly using K-profile parameterization of Large et al. (1994). Against lateral and bottom boundaries, free-slip boundary conditions are applied with quadratic bottom drag ($C_d = 2 \times 10^{-4}\,\mathrm{m^{-1}}$).

The tactic used to investigate the impact of the DWBC, coastline curvature, and continental slope geometry is to introduce artificial modifications to the ETOPO1 bathymetry. We refer to these as ''terraforming experiments.'' The model configuration for the terraforming experiments is otherwise identical to the control simulation. The control simulation and the terraforming experiments are initialized from the same initial conditions. Each simulation is spun up identically in two phases. In the first phase, a 2-yr integration is conducted with an additional lateral Laplacian diffusion in the momentum and tracer equations with diffusivity and viscosity of $200\,\mathrm{m^2\,s^{-1}}$. In the second phase of spinup, the Laplacian diffusion is turned off, and the model is integrated for an additional 4 yr. All of the results that are presented are from the following 5 yr of the model simulation.

b. *Separation metrics*

In this section, we describe the techniques used to determine where the Gulf Stream separates. The view taken here is that separation is the detachment of a three-dimensional current from a two-dimensional continental slope. Previous observational studies of the Gulf Stream position (e.g., Auer 1987; Gawarkiewicz et al. 2012) have been restricted to defining the position using two-dimensional surface metrics such as the sea surface temperature. This choice is constrained by the need for sufficient temporal and spatial resolution and timespan; currently satellite observations are the only observations that meet these criteria. Certainly, it is reasonable to think that there is a direct link between the northward penetration of surface water in the Gulf Stream and where it separates, but the details of such a connection has been rather vague in oceanographic literature. Given that the surface expression of the Gulf Stream in the Mid-Atlantic Bight is a primary concern for coupled atmosphere–ocean simulations and that there is an interest in uncovering the separation dynamics, we are motivated to characterize the separation of the Gulf Stream from the continental slope and illustrate the connection it has to the surface expression of the Gulf Stream postseparation.

The separation is described here using results from the control simulation. We first consider how the kinetic energy structure of the time-averaged Gulf Stream varies as it traverses the East Coast U.S. seaboard. The left panel of Fig. 3 shows the mean sea surface height for the control simulation with the Gulf Stream shaded in black. The Gulf Stream position is determined by the area between two SSH contours. These contours are chosen as $\eta_c \pm 25$ cm, where η_c is the SSH at 28°N where the surface Gulf Stream speed is a maximum. At 31°N, the Gulf Stream is seen turning northeast as it interacts with the Charleston Bump. Downstream of the CB, the continental slope steepens, indicated by the converging isobaths between 32° and 36°N in Fig. 2a. This region is referred to here as the convergence zone (CZ). Beyond the convergence zone, at the latitude of CH, the Gulf Stream makes a gradual northeast turn and heads OS.

Cross sections of mean kinetic energy are shown in the right panel of Fig. 3 at the four indicated locations. The thick, black contour marks KE $= 0.5\,\mathrm{m^2\,s^{-2}}$; we use the region within this contour to define the core of the Gulf Stream. Just south of the Charleston Bump and section CB, the core extends over 100 km laterally and down to 250-m depth. Within the core, kinetic energy in excess of $0.8\,\mathrm{m^2\,s^{-2}}$ penetrates as deep as 150 m. In contrast, the core is weakened downstream of the Charleston Bump at the start of the convergence zone. At Cape Hatteras, higher mean kinetic energy is seen within the core again but is not as intense as at CB. This is consistent with the high-resolution modeling study of Gula et al. (2015). They showed that mean kinetic energy is lost to eddy kinetic energy over the Charleston Bump, and eddy kinetic energy is transferred back to the mean between the Charleston Bump and Cape Hatteras within the convergence zone.

Offshore, the core is reduced in size and maximum mean kinetic energy, while the deeper kinetic energy structure is largely unchanged. This is consistent with the deceleration of the current and the descent of the vertical ''center of kinetic energy,'' defined as

$$z_c = \frac{\int Kz\,dA}{\int K\,dA}, \tag{2}$$

near the separation, where $K = (1/2)(u^2 + v^2)$ is the kinetic energy per unit mass associated with the lateral

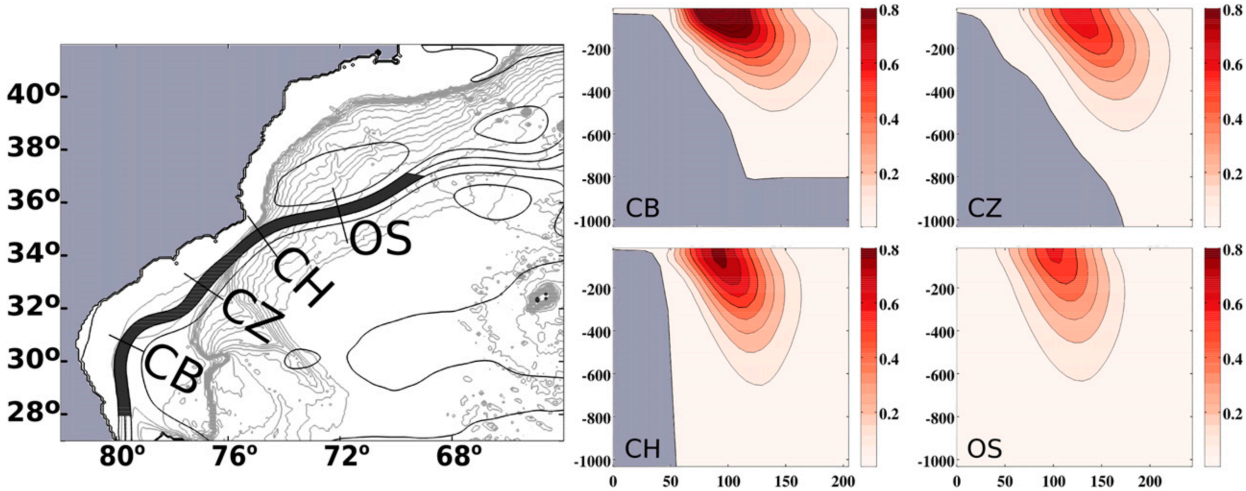

FIG. 3. The left panel shows contours of the mean sea surface height from the control simulation with the Gulf Stream pathway shaded in black. Cross sections of mean kinetic energy are shown in the right panel at the four indicated sections: CB, CZ, CH, and OS.

velocity field, z is the vertical coordinate, and the integration is conducted over the width of the Gulf Stream from the seafloor to the fluid surface. Figure 4 shows the vertical center of kinetic energy and the cross-sectional average of the depth underneath the Gulf Stream along the current's path. The depth underneath the Gulf Stream is shown for reference to indicate when the Gulf Stream crosses the continental slope, which occurs between 33° and 35°N. Since the Gulf Stream resides above 600 m (see the right panel of Fig. 3), it separates from the continental shelf in this region. Beyond 35°N (Cape Hatteras), the vertical center of mean kinetic energy descends by more than 50 m.

The "falling away" of the continental slope and the descent of the center of mean kinetic energy provide two symptoms of separation that can be compared to other metrics for directly detecting the Gulf Stream presence on the seafloor. When a boundary current separates, it implies that, just away from the boundary, the current has a nonzero component normal to the boundary. For an incompressible fluid, such a normal velocity is coincident with the convergence of flow in the boundary tangent plane. To illustrate this, let ξ_1 and ξ_2 denote the coordinate directions along the seafloor (the tangent plane), and let n denote the normal direction that points toward the fluid interior. Further, the velocity field can be rotated so that

$$\mathbf{u} = u_1\hat{\boldsymbol{\xi}}_1 + u_2\hat{\boldsymbol{\xi}}_2 + u_n\hat{\mathbf{n}}, \tag{3}$$

where u_1 and u_2 are the velocity components in the tangent plane, and u_n is the velocity component normal

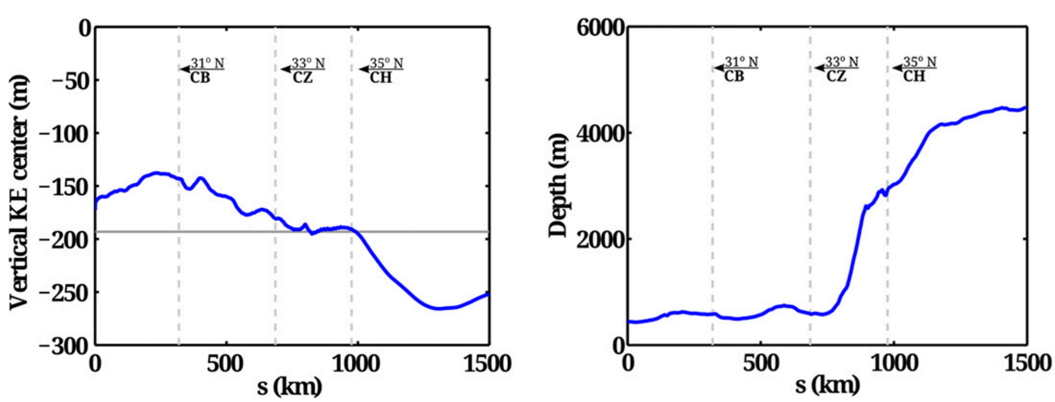

FIG. 4. The vertical center of (left) kinetic energy and the (right) depth underneath the Gulf Stream is shown as a function of the downstream distance along the Gulf Stream pathway. The drop in the vertical center of kinetic energy beyond Cape Hatteras is consistent with flow deceleration near the separation. The increase in the depth underneath the Gulf Stream between the convergence zone and Cape Hatteras indicates that the Gulf Stream is crossing the continental slope in this region.

to the boundary. The three orthonormal basis vectors in this rotated coordinate system are

$$\hat{\mathbf{n}} = (1 + \|\nabla h\|^2)^{-1/2}(h_x\hat{\mathbf{x}} + h_y\hat{\mathbf{y}} + \hat{\mathbf{z}}), \quad (4a)$$

$$\widehat{\xi}_1 = (\|\nabla h\|)^{-1}(-h_y\hat{\mathbf{x}} + h_x\hat{\mathbf{y}}), \quad \text{and} \quad (4b)$$

$$\widehat{\xi}_2 = \widehat{\xi}_1 \times \hat{\mathbf{n}}. \quad (4c)$$

From (4), the three velocity components in the rotated system are

$$u_1 = \mathbf{u}\cdot\widehat{\xi}_1 = (\|\nabla h\|)^{-1}(-uh_y + vh_x), \quad (5a)$$

$$u_2 = \mathbf{u}\cdot\widehat{\xi}_2 = (1 + \|\nabla h\|^2)^{-1/2}(\|\nabla h\|)^{-1} \times (uh_x + vh_y - w\|\nabla h\|^2), \quad \text{and} \quad (5b)$$

$$u_n = \mathbf{u}\cdot\hat{\mathbf{n}} = (1 + \|\nabla h\|^2)^{-1/2}(uh_x + vh_y + w). \quad (5c)$$

The incompressibility condition can be written in this coordinate system as

$$\nabla\cdot\mathbf{u} = \frac{\partial u_1}{\partial \xi_1} + \frac{\partial u_2}{\partial \xi_2} + \frac{\partial u_n}{\partial n} = 0. \quad (6)$$

Integration of (6) in the normal direction from the bathymetry toward the interior of the fluid over a distance Δn gives

$$u_n|_{n=\Delta n} \approx -\left(\frac{\partial u_1}{\partial \xi_1} + \frac{\partial u_2}{\partial \xi_2}\right)\Delta n, \quad (7)$$

where the no normal flow condition has been applied to the bathymetry. Note that to calculate the tangent plane divergence, the gradients of u_1 and u_2 are rotated appropriately:

$$\frac{\partial u_1}{\partial \xi_1} = \nabla u_1 \cdot \widehat{\xi}_1, \quad \text{and} \quad (8a)$$

$$\frac{\partial u_2}{\partial \xi_2} = \nabla u_2 \cdot \widehat{\xi}_2, \quad (8b)$$

where $\nabla = (\partial/\partial x)\hat{\mathbf{x}} + (\partial/\partial y)\hat{\mathbf{y}} + (\partial/\partial z)\hat{\mathbf{z}}$ is the gradient operator in (x, y, z) space.

Equation (7) shows how the fluid convergence in the tangent plane corresponds to a normal flow into the fluid interior and away from the boundary. Thus, the convergence of the boundary tangent flow implies the ejection of fluid parcels from the boundary and therefore can be an indicator of flow separation. This diagnostic is similar to those commonly used in engineering applications where phase plane analysis is conducted on the boundary tangent velocity field (Kenwright et al. 1999).

The unique physical properties of the Gulf Stream, particularly the temperature and salinity, leave an imprint of the Gulf Stream on the continental slope. A map of the temperature field on the seafloor can provide an additional indication of where flow detachment occurs, similar to the view of Stern (1998), who describes the separation as "a continual deflection of successive isopycnal layers off the slope and onto the isopycnals in the deeper ocean" Stern (1998, p. 2040). Figure 5 shows the mean bottom temperature and SST in the left panel and the bottom flow convergence with the SST and SSH in the right panel. Temperature signals are classified as cold (blue, $7°C < T < 15°C$), warm (orange, $15°C < T < 20°C$), and hot (red, $T > 20°C$). The north wall of the time-averaged Gulf Stream, in this paper, is set as the 22.5°C isotherm, as this is seen parallel to the SSH field from Cape Hatteras seaward. It is noted that this north-wall proxy is not problematic when analyzing a long time average ocean state, as is done here, but can be problematic for seasonally varying flow. The bottom temperature field on the continental shelf is characterized by warm and hot water, except for the cold-water intrusion over the Charleston Bump (32°N, 282°E). This cold-water intrusion is preceded by bottom flow convergence on the southern edge of the Charleston Bump that together indicates an early and temporary separation of the Gulf Stream from the continental shelf. It should be noted that this cold-water intrusion has been documented in observations. Sedberry et al. (2001, p. 5) report that "upwelling occurs mainly between 32° and 33°N, and it results from a deflection of the Gulf Stream offshore by the topographic irregularity of the Charleston Bump." This early separation, however, is not readily apparent in the SSH, as the Gulf Stream from the surface vantage point is still seen flowing along the continental slope. Just south of Cape Hatteras, the bottom hot-water signal is seen tapering off as the surface north wall and SSH indicate that the Gulf Stream is crossing the continental slope and heading seaward. Farther downstream, between 33° and 35°N, there is a clear signal in the bottom flow convergence that coincides with the region where the hot water tapers and the surface flow crosses the shelf. This is the site of the primary separation of the Gulf Stream.

When the Gulf Stream crosses the continental slope and separates, there is a net transport of fluid across isobaths. Schoonover et al. (2016) demonstrated that the dominant, large-scale balance in the barotropic vorticity budget in the Gulf Stream is primarily between the bottom pressure torque and planetary vorticity advection. On smaller scales, the vorticity budget can be modified by a "nonlinear torque" that incorporates, in part, the effect of transient eddies. Diagnostics produced from simulations in the Regional Ocean Modeling

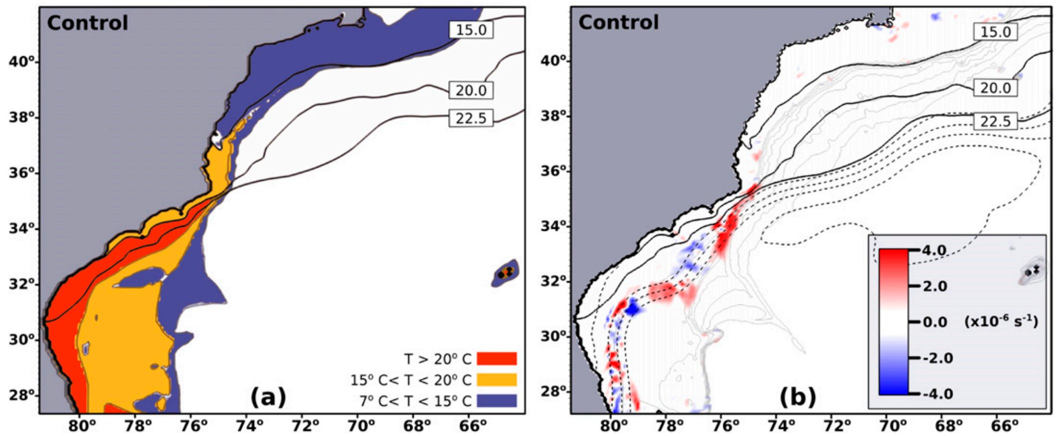

FIG. 5. (a) The mean seafloor temperature for the control simulation is shown in color with the SST contours in solid black. The hot and warm waters, with temperatures greater than 20°C and between 15° and 20°C, respectively, indicate the presence of the Gulf Stream along the inner continental slope and shelf. The tapering of the hot water at ≈35°N indicates the loss of contact of the Gulf Stream with the slope. (b) The mean bottom flow convergence field, SST (solid), SSH (dashed), and bathymetry (solid gray). The SSH is shown in increments of 25 cm and the bathymetry is in increments of 500 m.

System (ROMS; Shchepetkin and McWilliams 2005) and the MITgcm both indicated that the bottom pressure torque signal at the separation was markedly reduced in comparison to the upstream magnitude. The reduction of bottom pressure torque at the separation, where the Gulf Stream crosses isobaths, indicates a loss of topographic control on the fluid transport there. To illustrate how the bottom pressure torque can be reduced, the bottom pressure torque can be written in terms of a free-surface contribution and a baroclinic contribution:

$$J(P_b, h) = gJ(\eta, h) + J\left(\int_{-h}^{\eta} b\,dz, h\right), \qquad (9)$$

where the latter contribution is often referred to as the joint effect of baroclinicity and relief (JEBAR; Sarkisyan and Ivanov 1971; Holland 1972). Here, J denotes the Jacobian operator, P_b is the bottom pressure, $z = -h(x, y)$ defines the location of the seafloor, g is the acceleration of gravity, $z = \eta$ defines the position of the free surface, and b is the fluid buoyancy anomaly. A cancellation between the two contributions to the bottom pressure torque can result in a scenario consistent with the lack of topographic control of the transport. For this reason, JEBAR is a necessary part of the barotropic vorticity balance at the separation. It should be pointed out that JEBAR does not cause separation, but it is rather another symptom of the Gulf Stream separation as it crosses the continental slope. The JEBAR signal is intimately linked to the configuration of the velocity, stratification fields, and the local topography, and care must be taken in its interpretation [see Cane et al. (1998) for further discussion]. For JEBAR to be useful, there must be nontrivial flow on the topography. This describes the Gulf Stream, and we have found JEBAR to be a useful separation diagnostic.

Figure 6 shows the bottom temperature and salinity fields with the bottom flow convergence and bottom pressure torque along the path of the Gulf Stream. Both the bottom temperature and salinity fields show a noticeable decline between the convergence zone and Cape Hatteras, indicating that the Gulf Stream loses direct contact with the continental slope here. Within the same region, the localized bottom flow convergence field is seen in addition to a strong compensation between JEBAR and the free-surface contribution to the bottom pressure torque. These four metrics present a consistent picture of the Gulf Stream separation occurring between 33° and 35°N. The surface north wall of the Gulf Stream crosses the continental slope on the northern edge of the separation and proceeds northeastward into the Mid-Atlantic Bight. Upcoming experiments will look at changes to the separation and the surface expression of the Gulf Stream in this view due to modifications of the DWBC, coastline, and continental slope geometry.

3. Results

a. Deep western boundary current

The first experiment is designed to investigate the impact of the presence of the DWBC on the Gulf Stream separation. Normally, the DWBC crosses

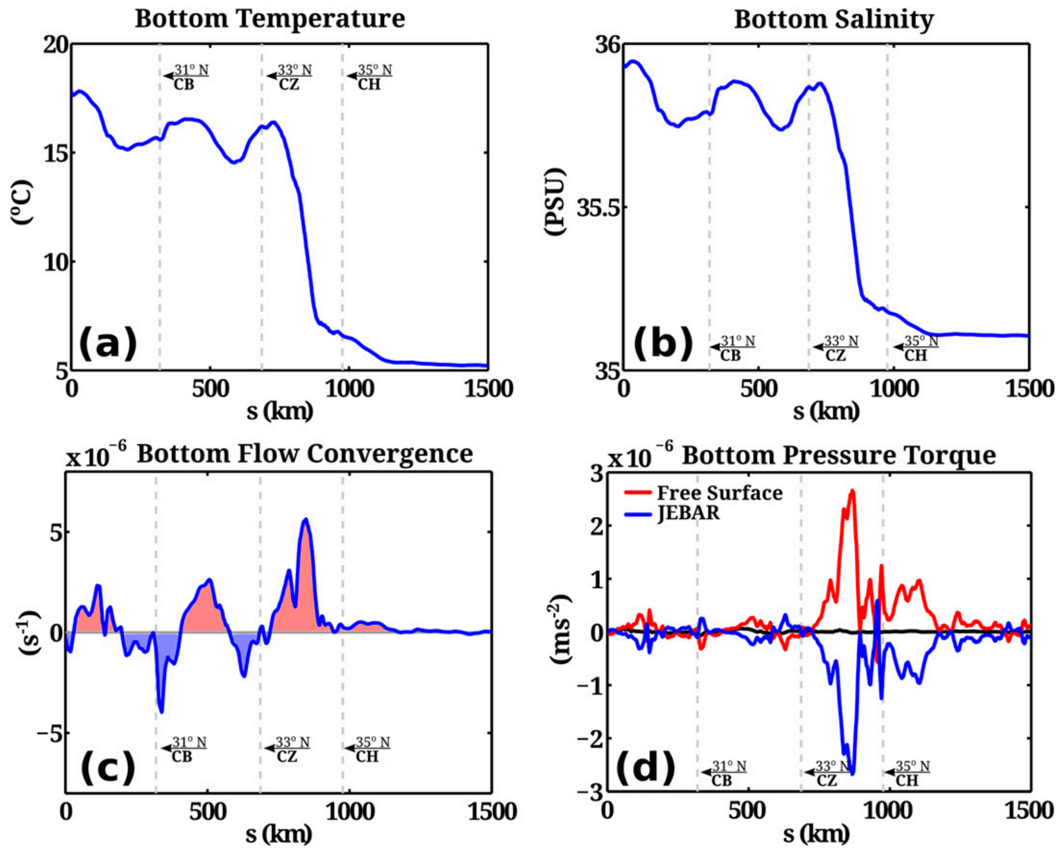

FIG. 6. The bottom (a) temperature, (b) salinity, (c) flow convergence, and (d) pressure torque are shown as a function of the downstream position of the Gulf Stream pathway for the control simulation. Regions corresponding to the Charleston Bump, convergence zone, and Cape Hatteras are indicated by the vertical dashed lines, corresponding to the locations marked in Fig. 3. Between the convergence zone and Cape Hatteras, separation of the Gulf Stream from the continental slope is observed in all four metrics. In the same region where the bottom temperature and salinity exhibit a substantial drop, there is a positive signal in the bottom flow convergence indicating fluid parcel ejection off of the shelf. Additionally, JEBAR is seen compensating the free-surface contribution to the bottom pressure torque, indicating a lack of topographic control on the fluid transport.

underneath the Gulf Stream around 36°N and descends down the deep continental slope (Fig. 7a). It has been suggested that the DWBC can locally influence the separation through two possible mechanisms. First, as the DWBC crosses underneath the Gulf Stream it can impart a southward momentum on the upper-layer Gulf Stream, limiting the northward penetration of the separation latitude. Second, the descending DWBC is purported to cause downwelling just offshore of Cape Hatteras that ‘‘stretches’’ the upper-layer Gulf Stream and is linked to flow deceleration (Tansley and Marshall 2000). These processes can be avoided entirely by preventing the DWBC from heading toward the usual crossover.

To steer the DWBC away from the usual crossover with the Gulf Stream, an artificial ridge is introduced in the Mid-Atlantic Bight that intercepts the DWBC near the inflow in the northeast corner of the basin (40°N, 294°E) and guides it southward, away from Cape Hatteras. The bathymetry for this experiment, shown in Fig. 2b, is otherwise identical to the control simulation bathymetry. The artificial ridge has a minimum depth of 1500 m so that it is not in direct contact with the Gulf Stream. The mean pressure field at 3000-m depth for the control simulation and the ‘‘blocking’’ experiment are shown in Fig. 7. The mean isobars effectively mark streamlines for the DWBC. In the control simulation (Fig. 7a), the DWBC enters into the domain around 40°N with a southwestward heading. It crosses underneath the Gulf Stream offshore of Cape Hatteras (around 36°N), where it can be seen turning offshore before part of it rejoins the continental slope. Figure 7b shows that the DWBC is successfully prevented from reaching the usual crossover point with the Gulf Stream in the blocking experiment. Instead, the DWBC forms a recirculation to the east of the ridge and the remaining portion of the

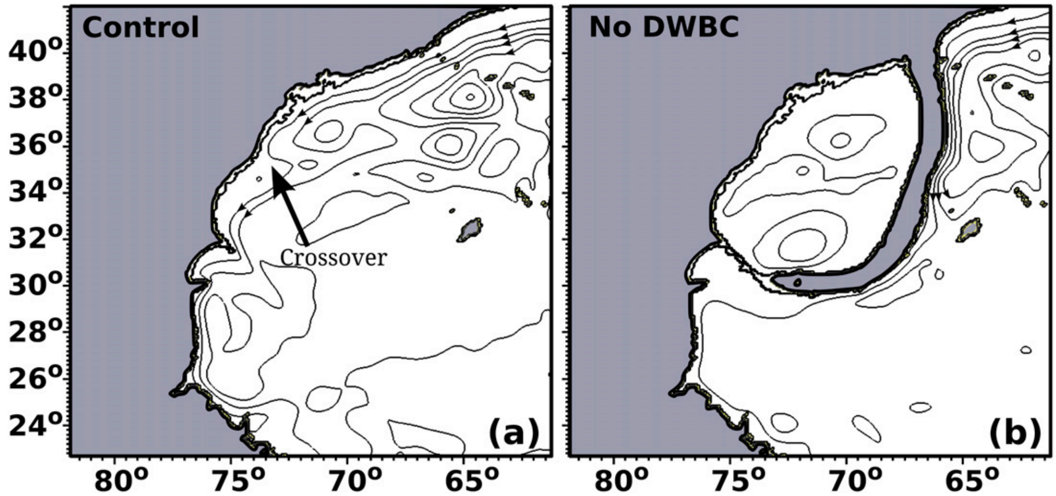

FIG. 7. The mean pressure field (contours) for (a) the control simulation and (b) the DWBC blocking experiment is shown at 3000-m depth. In the control simulation, the DWBC is seen flowing southwestward at 40°N, parallel to the 3000-m isobath until it reaches 36°N where it crosses underneath the Gulf Stream. In the blocking experiment, the artificial ridge successfully intercepts the DWBC and guides it toward the Blake Ridge, away from the usual crossover with the Gulf Stream, thus avoiding local interactions with the Gulf Stream. The pressure contours are shown in increments of 2.5 $m^2 s^{-2}$ in both panels.

current flows southward along the artificial ridge until it is rejoined with the continental slope just south of the Blake Ridge.

The bottom temperature field and SST are shown in Fig. 8a. The bottom temperature signal on the continental shelf is nearly identical to the control simulation with the hot water tapering off just south of Cape Hatteras. The bottom separation metrics along the Gulf Stream path for this experiment are shown in Fig. 9. The diagnostics indicate that separation from the continental slope still occurs between 33°N and Cape Hatteras, consistent with the results of the control simulation. This indicates that the DWBC is not fundamental to the separation latitude of the Gulf Stream.

Thompson and Schmitz (1989), Zhang and Vallis (2007), Hurlburt and Hogan (2008), and Hurlburt et al. (2011) all found a sensitivity of the Gulf Stream interior pathway to the strength of the DWBC transport. We agree that the interior pathway is sensitive to the DWBC (this is apparent in Fig. 8); however, the separation latitude is unaffected. Zhang and Vallis (2007) found that the DWBC strength directly influences the strength of the northern recirculation gyre, which can in turn alter the interior pathway of the separated Gulf Stream. A weak DWBC causes a weak northern recirculation gyre that ultimately results in a northward displacement of the interior Gulf Stream pathway. In Zhang and Vallis (2007), it is

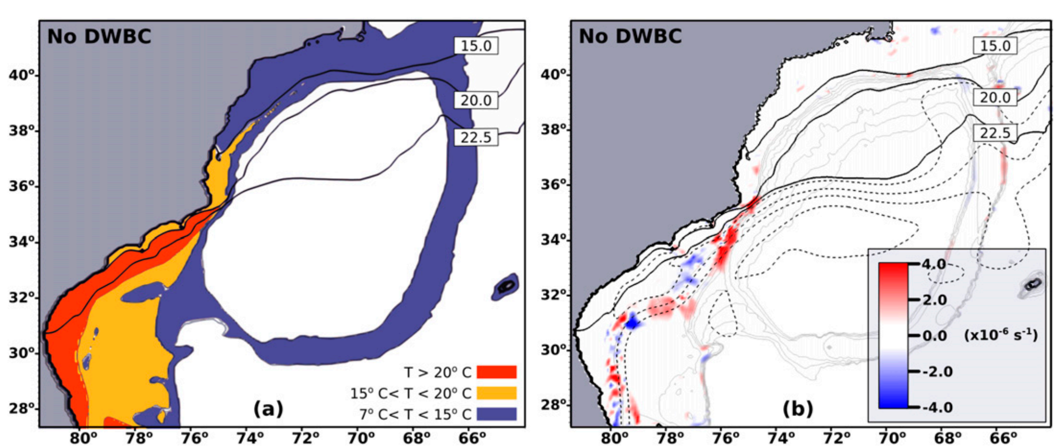

FIG. 8. As in Fig. 5, but for the blocked DWBC experiment.

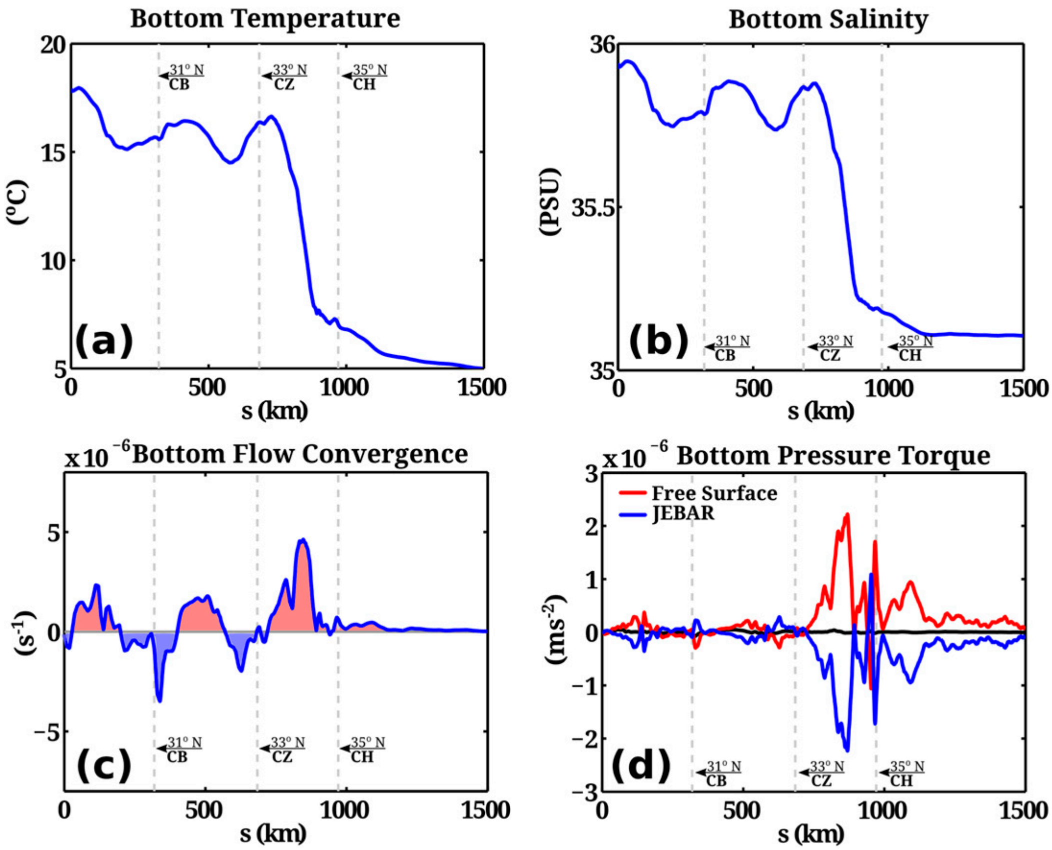

FIG. 9. As in Fig. 6, but for the blocked DWBC experiment. The separation without a DWBC is broadly consistent with the control simulation.

difficult to say where separation occurs, given their 1° resolution. In all of their experiments, though, it is roughly at 40°N, well beyond the observed separation, despite changes in the Gulf Stream interior pathway. Their results are reminiscent of regional simulations of Thompson and Schmitz (1989). In all of the experiments in Thompson and Schmitz (1989), the Gulf Stream remained attached to the western boundary beyond Cape Hatteras, despite the sensitivity of the interior pathway. Again, these are consistent with our findings. We have examined a specific topographic modification, and while the Gulf Stream interior pathway is affected, we cannot make more definitive statements than this.

b. Coastline curvature

The steadiness of the separation latitude near Cape Hatteras has motivated many authors to hypothesize that local topography exerts a leading-order control on the separation process. A coastal promontory like Cape Hatteras, or more generally the coastline curvature, has been suggested to be a necessary ingredient for separation (Dengg 1993; Ozgokmen et al. 1997; Munday and Marshall 2005). Often, this is described as the coast leaving the Gulf Stream rather than the Gulf Stream leaving the coast. To test this idea, the coastline and inner continental slope of the eastern United States is modified to remove the sharp turn around Cape Hatteras. The bathymetry for this experiment, dubbed No Hatteras, is shown in Fig. 2c. Clearly, the promontory in the coastline is absent, and the large-scale curvature in the shallower isobaths has been reduced in comparison to the control bathymetry.

Again, the mean bottom temperature, SST, bottom flow convergence, and SSH fields are shown in Fig. 10 for the No Hatteras experiment. The bottom temperature field on the continental shelf and slope exhibits some differences that are mainly due to the coastal and continental slope modification. Hot and warm waters are seen permeating the shallow (<500-m depth) region of the continental shelf with warm waters reaching as far north as 38°N. However, the hot water is still seen tapering off around 35°N near the bottom flow convergence signal at the shelf edge, similar to the control simulation. The surface Gulf Stream, indicated by the SSH and north wall (right panel, Fig. 12), is seen heading offshore around 36°N at the

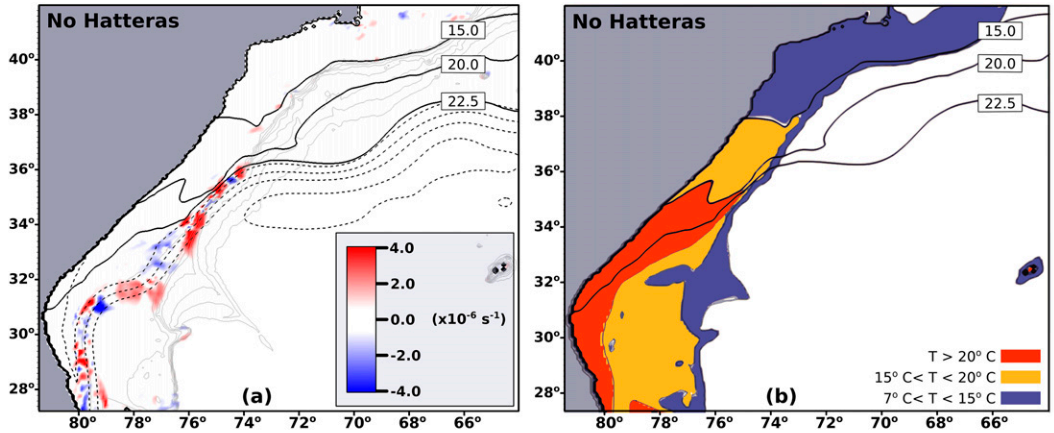

FIG. 10. As in Fig. 5, but for the No Hatteras experiment.

former location of Cape Hatteras and is almost identical to the control simulation. The bottom separation metrics for this experiment are shown in Fig. 11. The bottom fields underneath the Gulf Stream indicate that separation occurs between the convergence zone and Cape Hatteras, consistent with the control simulation and the blocked DWBC experiment. This experiment suggests that the coastline curvature does not have a considerable impact on the Gulf Stream separation.

c. Continental slope geometry

Notice that, in all of the simulations shown, the separation occurs where the continental shelf

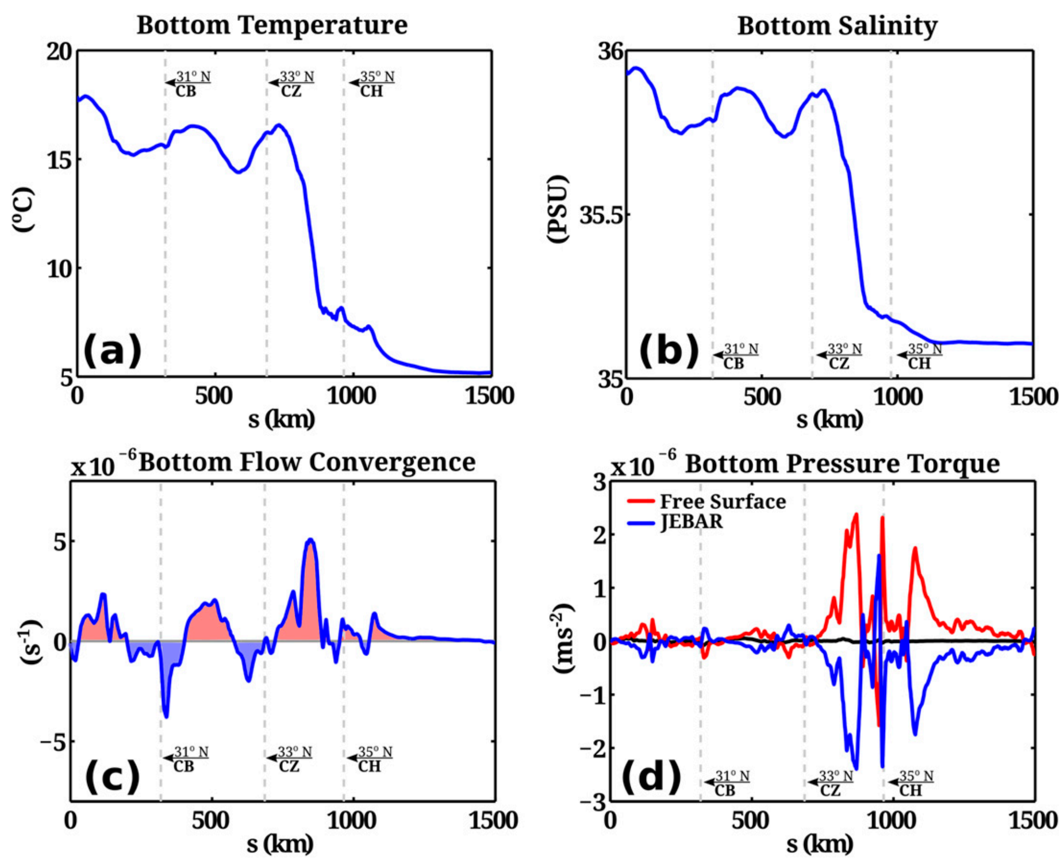

FIG. 11. As in Fig. 6, but for the No Hatteras experiment. The separation without Cape Hatteras is broadly consistent with the control simulation.

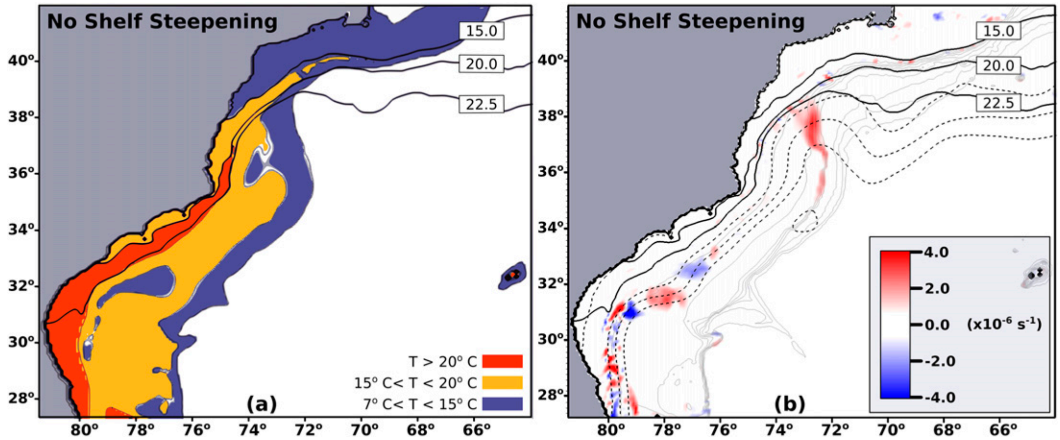

FIG. 12. As in Fig. 5, but for the experiment where the shelf steepening is removed.

steepens, just south of Cape Hatteras. Stern (1998) suggested that the steepening of the continental shelf is of primary importance for the separation process. His hypothesis is tested here by maintaining the continental shelf width around Cape Hatteras and effectively moving the ''steepening zone'' into the Mid-Atlantic Bight. The bathymetry for this experiment is shown in Fig. 2d. The isobaths around Cape Hatteras are spread out and maintained parallel to each other, indicating that the steepening of the continental shelf has been removed. Figure 12 shows the mean bottom and surface fields for this experiment. Clearly, Gulf Stream waters are observed beyond Cape Hatteras, reaching 37°N. Hot water penetrates farther north into the Mid-Atlantic Bight both along the inner slope and at the surface. The north wall and SSH indicate that the penetration of the hot and warm SST is directly linked to the mean pathway of the Gulf Stream. Figure 13 shows the bottom separation diagnostics along the path of the Gulf Stream. In this experiment, the drop in the bottom temperature and salinity occurs north of Cape Hatteras, indicating that the separation has been displaced northward. Further, the bottom flow convergence and JEBAR compensation signals south of Cape Hatteras are almost completely removed, and the signals associated with the primary separation are found north of Cape Hatteras near the new location of the shelf steepening. It is important to point out that the Gulf Stream separation moved due to the change in the boundary conditions, which together leads to a different signal for the JEBAR diagnostic. This does not imply that the change in the JEBAR signal caused a change in the separation. Rather, our knowledge of the Gulf Stream structure and the nature of its detachment from the continental shelf allow us to use this as another diagnostic for separation location. This experiment indicates that removing the steepening of the continental shelf has a substantial impact on the separation latitude and the surface penetration of the Gulf Stream and associated temperature signal.

The set of experiments presented here indicate that the details of the continental slope geometry are important. The bottom metrics that are used to estimate the separation location produce consistent signals, even in the last experiment where the separation is displaced north of Cape Hatteras. Although the amplitude of the bottom flow convergence and JEBAR are not as strong in this experiment, we argue that the metrics used to detect separation are robust and indicate that separation occurs where the shelf steepens, even when the steepening zone is displaced. Symptoms of the Gulf Stream separation include the decrease in the temperature and salinity field along the bottom underneath the current, convergence of boundary flow in the tangent plane, and compensation between the free-surface and baroclinic contributions to the bottom pressure torque.

4. Discussion

a. Stern's model, shelf waves, and the JEBAR symptom

The terraforming experiments suggest that the most significant factor controlling the Gulf Stream separation, of those examined here, is the steepening of the continental shelf. This feature is abrupt and unambiguous and by far the more remarkable feature in the geometry of the western boundary in this region. Coastline and slope curvature and the presence of the DWBC are shown to have a minimal impact on the separation latitude and the northward penetration of the mean surface Gulf Stream position. These results are most

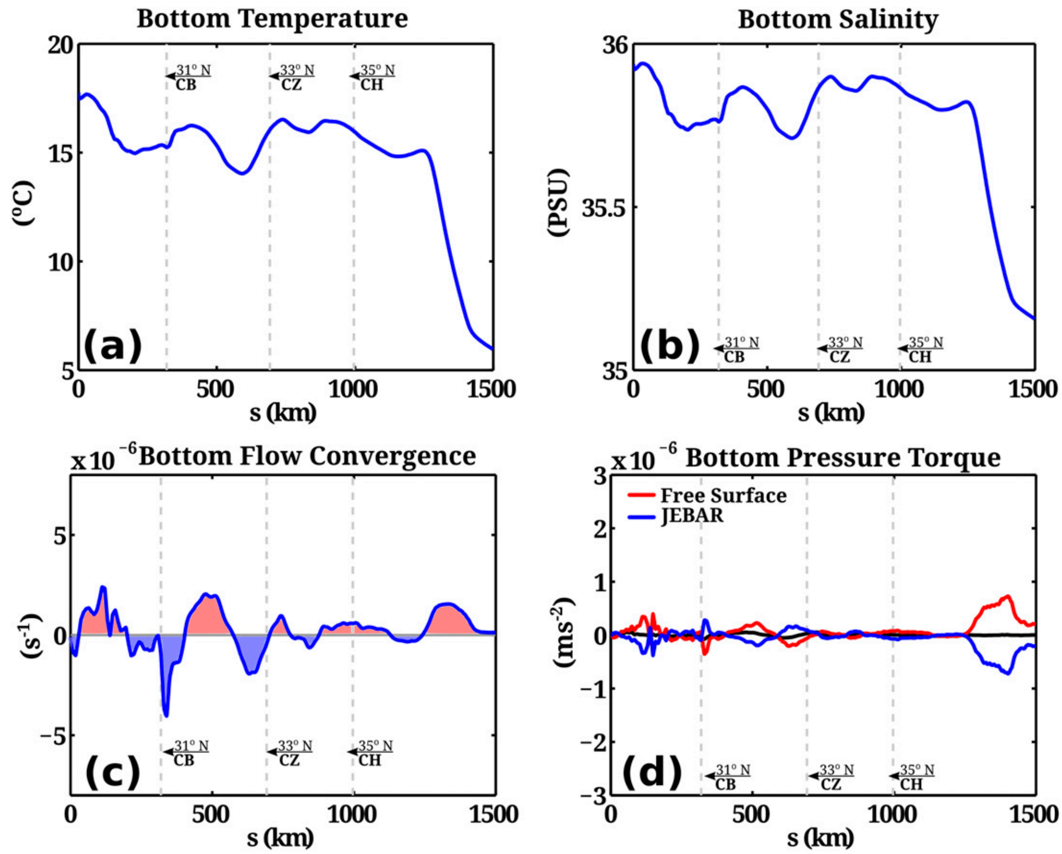

FIG. 13. As in Fig. 6, but for the experiment where the shelf steepening is removed. Notice that the separation has moved to a location south of the new convergence zone.

consistent with the separation theory of Stern (1998) and therefore motivate a more detailed study of Stern's model of the Gulf Stream separation. We outline Stern's model here and illustrate the need for further extensions to include continuous stratification and nonlinearities. Additionally, we examine how his theory can lead to the reduction of the bottom pressure torque at the separation, illustrating that this metric is a result of the configuration of the flow detachment from topography and does not cause separation.

Figure 1 provides a schematic for the setup of the Stern model. He adopted a 1.5-layer model where a parallel shear flow was partly over the topography and partly over the fluid interface. Inshore of the incropping, in the barotropic region, the equations of motion are taken to be the steady-state, rigid-lid, shallow-water equations. At the incropping, a boundary condition is used that ensures fluid parcels exiting the barotropic region conserve kinetic energy and thickness. Stern makes two simplifying assumptions:

1) The continental slope is dominantly varying in the cross-stream direction and steepens only by a small factor ε in the downstream direction. The bathymetry is mathematically expressed as

$$z = -[\overline{h}(x) + \varepsilon h'(x, y)], \tag{10}$$

where x is the cross-stream direction, and y is the along-stream direction.

2) The cross-slope length scales L_x are smaller than the along-slope length scales L_y by a factor of ε:

$$\frac{L_x}{L_y} \sim O(\varepsilon), \tag{11}$$

which is commonly referred to as the long-wave assumption.

Solutions are found using a perturbation expansion in orders of ε. The $O(\varepsilon)$ balance indicates that the steepening results in a source of cyclonic vorticity caused by the leading-order flow crossing isobaths. This source of vorticity acts as a forcing term that generates a spectrum of barotropic shelf dynamics that are affected by the mean flow (Hughes 1986). For a current speed slower than the barotropic shelf wave speed (subcritical flows), a steepening shelf results in mass transport onto the slope, and the flow remains attached to the boundary. Critical and supercritical flows (i.e., flows at or faster than the shelf wave speed) are found to result in offshore transports and a separated current when encountering a steepening shelf.

Stern's model is unique in that it joins a barotropic fluid to a 1.5-layer fluid through a ''novel'' boundary condition that implies conservation of kinetic energy and fluid parcel thickness across the incropping line. In this way, it is not entirely a barotropic theory. Separation in the Stern model is observed as a cross-isobath flow associated with a deceleration of the inshore flank of the modeled Gulf Stream. At the incropping, the momentum balance is

$$\overline{v}v'_y + (f + \overline{v}_x)u' = (g\eta'_I)_y, \tag{12}$$

where $\overline{v}(x)$ is the leading-order, along-slope velocity component; v' is the $O(\varepsilon)$ correction; f is the Coriolis parameter; u' is the cross-slope velocity component; g is the acceleration of gravity; and η'_I is the displacement of the isopycnal surface.

The inshore flank of the background flow (the modeled Gulf Stream) is such that $\overline{v} > 0$ and $\overline{v}_x > 0$. When separation occurs, $u' > 0$ at the incropping. Provided $v'_y \geq 0$ at the incropping (a possible scenario given the requirement of cyclonic vorticity generation), the isopycnal position is predicted to increase with downstream position. The slope in the isopycnal along the topographic slope corresponds to a baroclinic pressure gradient along isobaths, that is, the presence of JEBAR.

b. Continuously stratified Stern model

Stern's model relies on a steepening shelf to instigate shelf wave production. Our final experiment is consistent with the notion that we removed the primary feature associated with the generation of shelf waves that interact with the Gulf Stream and lead to flow separation. The validity of Stern's model becomes suspect if the isopycnal slope exceeds the topographic slope at the incropping; beyond the shelf steepness, the equations are no longer valid. The isopycnal slope at the incropping is related to the leading-order flow speed through geostrophy:

$$\eta'_x = \frac{f\overline{v}}{g'}, \tag{13}$$

where $z = -H + \eta'$ is the depth of the isopycnal, H is a reference depth, $\overline{v}$ is the leading-order flow speed, and f is the Coriolis parameter. The reduced gravity due to the stratification is $g' = (g\delta\rho)/\rho_0$, where $\delta\rho$ is the density discontinuity, and ρ_0 is a reference density. If the isopycnal slope is restricted to be smaller than the topographic slope, then

$$\frac{\eta'_x}{\overline{h}_x} = \frac{f\overline{v}}{g'h_x} = \frac{\overline{v}}{c} < 1, \tag{14}$$

where

$$c \equiv \frac{g'h_x}{f} \tag{15}$$

is the baroclinic topographic Rossby wave speed. Taking values typical for the midlatitude North Atlantic, $\delta\rho \sim 1\,\mathrm{kg\,m^{-3}}$, $g \sim 10\,\mathrm{m\,s^{-2}}$, $f \sim 10^{-4}\,\mathrm{s^{-1}}$, and $h_x \sim 0.01$, we get $c \sim 1\,\mathrm{m\,s^{-1}}$. This speed is on the order of the typical Gulf Stream speed suggesting interactions with baroclinic waves are possible. Extensions to continuous stratification are likely to yield richer relevant dynamics.

Key to Stern's theory is the need for the Gulf Stream to arrest local topographic waves. To see if this criterion is met in a continuously stratified fluid, we now examine the wave dynamics that follow from a baroclinic extension of Stern's model. The inviscid and adiabatic hydrostatic primitive equations permit the conservation of Ertel's potential vorticity following fluid parcels:

$$Q_t + uQ_x + vQ_y + wQ_z = 0, \tag{16}$$

where u, v, and w are the velocity field components. The potential vorticity Q is related to the velocity field and buoyancy b through

$$Q = (v_x - u_y + f)b_z + u_z b_y - v_z b_x. \tag{17}$$

In a similar fashion to Stern's model, the velocity field is broken into an along-slope geostrophic flow and an $O(\varepsilon)$ correction that results from the slight steepening in the slope. Applying the long-wave assumption allows the potential vorticity to be expressed solely in terms of pressure p':

$$Q = \overline{Q} + \varepsilon Q' = f\overline{b}_z + \varepsilon\left(fp'_{zz} + \frac{\overline{b}_z}{f}p'_{xx}\right) + O(\varepsilon^2). \tag{18}$$

To $O(\varepsilon^2)$, the potential vorticity balance [(16)] reduces to

$$Q'_t + \overline{v}Q'_y + w'\overline{Q}_z = 0, \tag{19}$$

where the along-slope flow is assumed uniform. The cross-slope and vertical velocity components can be obtained from the meridional momentum and buoyancy equations, respectively:

$$u' = -\frac{1}{f^2}(fp'_y + p'_{xt} + \overline{v}p'_{xy}) \quad \text{and} \tag{20a}$$

$$w' = -\frac{1}{N^2}(p'_{zt} + \overline{v}p'_{zy}). \tag{20b}$$

Substituting (20b) into (19) and applying separation of variables

$$p'(x,y,z,t) = \psi(x,z)\phi(y,t) \tag{21}$$

results in an elliptic equation for the cross-shelf pressure field:

$$\psi_{xx} + \left(\frac{f^2}{\overline{b}_z}\psi_z\right)_z = 0. \tag{22}$$

Along the seafloor, the no normal flow boundary condition

$$u'\overline{n}_x + w'\overline{n}_z = 0, \quad \text{at} \quad z = -\overline{h}(x), \tag{23}$$

becomes

$$\phi_t + (\overline{v} - c)\phi_y = 0, \quad \text{and} \tag{24a}$$

$$\psi_x\overline{n}_x + \frac{f^2}{N^2}\psi_z\overline{n}_z = -\frac{f}{c}\psi\overline{n}_x, \quad \text{at} \quad z = -\overline{h}(x), \tag{24b}$$

through the use of (20) and separation of variables as in (21). The components of the outward pointing boundary normal vector are $\overline{n}_x$ and $\overline{n}_z$. The free-wave speed c is an eigenvalue that results from the separation of variables applied to the no normal flow boundary condition. Equation (24a) reveals that the topographic wave speed in a uniform geostrophic flow is Doppler shifted by the flow speed, indicating that arrest is possible if $\overline{v} = c$.

To obtain the free-wave speed c and determine if arrest is possible for the Gulf Stream, additional boundary conditions are needed. At the fluid surface ($z = 0$), the rigid-lid condition is enforced,

$$\psi_z = 0 \quad \text{at} \quad z = 0, \tag{25}$$

and far from the continental slope, the pressure decays to zero so that the solution is bounded:

$$\psi \to 0, \quad \text{as} \quad x \to \infty. \tag{26}$$

Together, (22), (24b), (25), and (26) result in an eigenvalue problem for the topographic wave modes and the wave speeds. For an arbitrary topographic profile, it is difficult to solve for the cross-shelf wave modes and speeds analytically. Instead, the boundary value problem is discretized using the continuous Galerkin spectral element method. Discretization results in a generalized eigenvalue problem

$$c\mathbf{Ap} = \mathbf{Wp}, \tag{27}$$

where $\mathbf{A}$ is the discrete form of the potential vorticity operator [(22)], and $\mathbf{W}$ is the discrete form of the boundary condition along the topography [(24b)]. The eigenvalues and eigenmodes of (27) approximate the wave speeds and the wave modes for the continuous problem, respectively. Although the discrete problem permits M possible wave modes (where M is the number of degrees of freedom), the implicitly restarted Arnoldi method (Lehoucq and Sorensen 1996) is used to efficiently estimate only a subset of the eigenpairs.[1]

As an example,

$$\overline{h}(x) = h_0\left\{1 - \left[\tanh\left(\frac{2x}{L_1}\right) + \tanh\left(\frac{2x - x_0}{L_2}\right)\right]\right\} \tag{28}$$

defines an idealized cross-flow topographic profile similar to that observed between Charleston Bump and Cape Hatteras. Here, $h_0 = 1000\,\text{m}$, $L_1 = 100\,\text{km}$, $L_2 = 50\,\text{km}$, and $x_0 = 100\,\text{km}$. Additionally, the Coriolis parameter is set to $f_0 = 10^{-4}\,\text{s}^{-1}$ and $\overline{b}_z = 10^{-4}\,\text{s}^{-2}$, and the 10 fastest wave modes are extracted. The wave speeds for this setup are shown in the left panel of Fig. 14. It can be seen that modes 6 through 10 have speeds between 1 and $2\,\text{m}\,\text{s}^{-1}$, indicating that arrest of higher-order modes by the Gulf Stream is possible under continuous stratification. This illustrates that Stern's separation theory is still plausible under a stratified extension. The pressure field associated with mode 7 is shown in the right panel of Fig. 14. The length scales of the pressure disturbances associated with this mode are $O(50)$ km, which is similar to the width of the Gulf Stream. The arrest of such a wave would likely produce disturbances in the total pressure field on length scales of the Gulf Stream width further underscoring the importance of interactions with topographic waves.

The dispersion relation calculated from the idealized topography and stratification setup suggests that wave arrest, a key ingredient in Stern's separation theory, is possible. However, confirmation of separation by wave arrest requires further investigation. The sensitivity of the wave mode structures and speeds to variable stratification and changes in the topography is needed to provide further confidence in this theory. Additionally, the Gulf Stream jet is more complex than a uniform geostrophic flow that was assumed here, and it is likely

[1] The software for computing the topographic wave modes can be found at www.github.com/schoonovernumerics/SELF-v3.0.

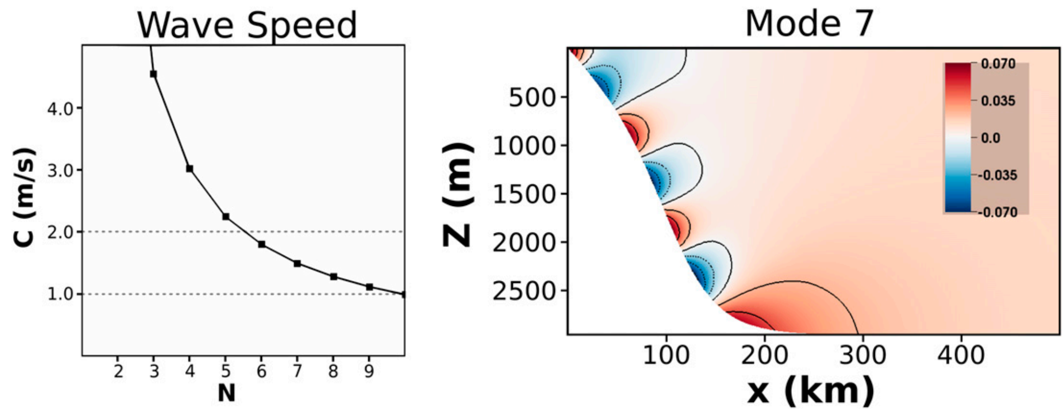

FIG. 14. (left) The free topographic wave speeds are shown as a function of the wave mode number for $f_0 = 10^{-4}\,\mathrm{s}^{-1}$ and $N^2 = 10^{-4}\,\mathrm{s}^{-2}$ with the shelf profile given in (28). The gray dashed lines indicate wave speeds between 1 and 2 m s^{-1}, typical of the Gulf Stream speed. (right) The cross-shelf pressure field is shown for mode 7. The length scales of the pressure disturbances for this wave mode are $O(50)$ km, further supporting the hypothesis that interactions between the Gulf Stream and these waves are important.

that a variable background flow will result in a more complicated connection between separation and the arrest of topographic waves. In Stern's original model, arrest was associated with resonant production of cyclonic vorticity that inherently leads to a breakdown in the linearization employed in his model (and the one presented here). It is currently unclear how the Gulf Stream and topographic wave interactions would progress with the inclusion of nonlinearities, though it would be necessary to clarify these details given that it is likely the Gulf Stream regularly interacts with these disturbances.

c. Separation recipe

The experiments shown here demonstrate the importance of the continental slope geometry along the western boundary of the North Atlantic basin. In agreement with the Stern model, we find the steepening of the slope between the Charleston Bump and Cape Hatteras chooses the location of the Gulf Stream separation. The experiments alone indicate that care must be taken in the representation of the bathymetry in this region. Ezer (2016) similarly concludes poor vertical resolution can result in poor Gulf Stream separation. Stern's theory indicates that the continental slope steepening and the waves that result from interactions between the Gulf Stream and the variable slope are necessary to obtain separation. Together, our results and Stern's theory imply that both the accurate representation of the slope steepening near Cape Hatteras and the shelf wave field are necessary for achieving proper separation.

Excessive smoothing or insufficient resolution of the bathymetry can weaken the effective continental slope steepening and may inhibit the growth of shelf waves. Let τ and s denote the across- and along-isobath directions, respectively. The increase in the bathymetric gradient magnitude along an isobath provides a measure of the shelf steepening and can be calculated as

$$\varepsilon = \frac{\partial}{\partial s}(\|\nabla h\|). \tag{29}$$

In practice, (29) is calculated by using the formula

$$\varepsilon = \nabla(\|\nabla h\|) \times \nabla h \tag{30}$$

to estimate the change in the steepening along an isobath.

To demonstrate that a coarse-resolution simulation may underestimate the magnitude of the shelf steepening, (30) is estimated using the control bathymetry and a smoothed version of the control bathymetry. Figure 15 depicts (29) for the control bathymetry and a smoothed version of the control bathymetry. Convolution with a Gaussian kernel (half-width of 100 km) is used to obtain the smoothed bathymetry. The top two panels of Fig. 15 indicate that the smoothed bathymetry underestimates the magnitude and structure of the steepening field. The bottom panel depicts this metric along the lines shown in the upper panels, with the solid black and dashed gray lines corresponding to the control and smoothed bathymetry, respectively. The smoothed bathymetry is shown to produce a steepening that is orders of magnitude smaller than the control. It is plausible that coarse resolution, or excessive smoothing, can weaken the Gulf Stream interaction with the slope that is necessary for causing separation by weakening the continental slope steepening, a key ingredient of Stern's model. To

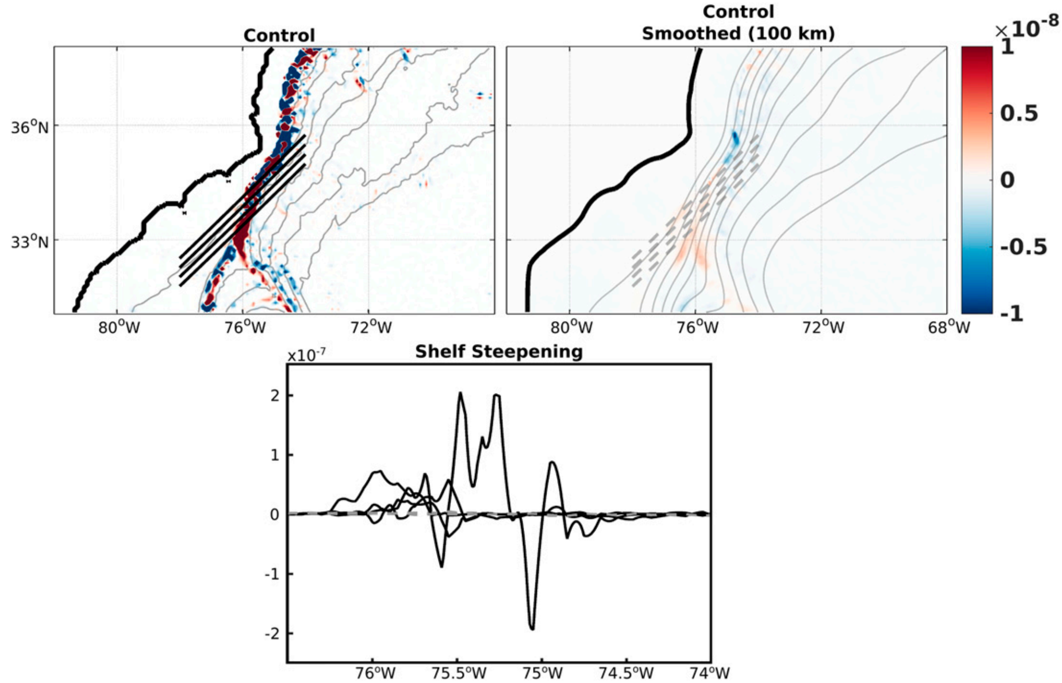

FIG. 15. The steepening metric, calculated from (29), is shown in color for (top left) the control bathymetry and (top right) the control bathymetry smoothed by a Gaussian filter with a half-width of 100 km. Isobaths are shown in solid gray with contour intervals of 500 m. (bottom) The steepening metric is interpolated onto the solid black lines in the top-left panel and the dashed gray lines in the top-right panel. The solid black lines and gray dashed lines are located at the same locations but are used to delineate the metric from the control bathymetry (solid black) and smoothed bathymetry (dashed gray). The smoothed topography here represents the bathymetry in a coarse-resolution ocean model. Note that the steepening metric, according to (29), is unitless.

achieve proper separation in a coarse-resolution simulation, it is likely that information about the subgrid-scale continental slope will need to be included.

The primary subgrid-scale parameterizations of unresolved eddy activity in GCMs are Laplacian and biharmonic momentum, heat, and salt diffusion. When applied to the momentum equations, both operators remove energy from the flow and do so more effectively at smaller length scales. For illustrative purposes, a Fourier transform of

$$\mathbf{u}_t = \nu\nabla^2\mathbf{u} \tag{31}$$

gives the transfer function as

$$\frac{K(t)}{K_0} = e^{-2\nu\|\mathbf{k}\|^2 t}. \tag{32}$$

The quantity $K(t)$ is the kinetic energy of the velocity field $\mathbf{u}$ at time t, K_0 is the kinetic energy at some initial time, and the eddy viscosity is ν. The Gulf Stream flow over the steepening slope results in an energy transfer from the Gulf Stream to a spectrum of shelf waves that may also experience a loss of energy due to the diffusion operator. Suppose that the Gulf Stream–slope interaction results in the growth of shelf wave energy over a time scale T_{growth}. Energy is lost from the wave over a time scale that corresponds to its wavenumber:

$$T_{\mathrm{lap}} = (\nu\|\mathbf{k}\|^2)^{-1}. \tag{33}$$

If the time scale for energy loss T_{lap} is shorter than the time scale for wave growth T_{growth}, then the shelf waves lose energy faster than they are given energy from the flow interaction with topography. To achieve proper separation, the shelf waves must be present. Thus, it is necessary that the shelf wave growth time scale remains smaller than the dissipation time scale:

$$\frac{T_{\mathrm{growth}}}{T_{\mathrm{lap}}} = \nu\|\mathbf{k}\|^2 T_{\mathrm{growth}} < 1. \tag{34}$$

Equation (34) provides a bound for the (Laplacian) eddy viscosity that permits the growth of shelf waves. Biharmonic momentum diffusion results in a similar condition:

$$\frac{T_{\mathrm{growth}}}{T_{\mathrm{bih}}} = \nu_4\|\mathbf{k}\|^4 T_{\mathrm{growth}} < 1. \tag{35}$$

For a given wavenumber and growth time scale, increasing the eddy viscosity may violate the separation conditions of (34) or (35). Additionally, the separation conditions are in qualitative agreement with the eddy-resolving modeling study of Bryan et al. (2007), who found that excessively large eddy viscosity can disrupt the Gulf Stream separation, often leading to a northward migration of the separation latitude.

The conditions from (34) and (35) provide testable statements about the nature of the separation, provided the knowledge of the separation-relevant shelf wavenumbers and growth rates is available. The Stern model, however, does not provide this information directly. This motivates further investigation of the Stern model and the underlying shelf wave dynamics. An understanding of the energetic balances between the Gulf Stream and shelf waves and the impact of subgrid-scale parameterizations, such as Laplacian or biharmonic diffusion, will provide the necessary details to explain the sensitivities of the separation to model configurations. Without knowledge of the wavelengths and growth rates of the shelf waves involved, (34) provides only a qualitative indication that an upper bound on the eddy viscosity should exist in order to achieve proper separation. Extensions of the Stern model and the underlying shelf wave theory is needed to provide a quantitative upper bound that can be used to verify the Stern hypothesis and (if correct) guide future model configuration.

5. Conclusions

Regional terraforming experiments within the MITgcm suggest that the Gulf Stream separation is insensitive to the presence of the DWBC and the curvature in the coastline. In contrast, removing the steepening in the continental slope between the Charleston Bump and Cape Hatteras provided an effective means for producing a northward separation. These results are most consistent with the theory of Stern (1998), who suggested that interactions between the Gulf Stream and local shelf waves generated by the steepening are important. Separation by wave arrest supplies a reasonable explanation for both the northward separation problem in coarse-resolution models and the separation latitude sensitivity to subgrid-scale parameterizations. We argue that coarse-resolution [$O(100)$ km] models consistently produce poor separation because they cannot accurately represent the shelf steepening around Cape Hatteras. Additionally, it may be that the waves involved in the separation process are, at best, marginally resolved and are likely damped by numerical dissipation or subgrid-scale parameterizations. This claim is subject to a verification of the Stern hypothesis and motivates the investigation of baroclinic and nonlinear extensions of Stern's model.

Acknowledgments. Funding for this research was provided by NSF under Award OCE-1049131. J. Schoonover gratefully acknowledges the support of the U.S. Department of Energy through the LANL/LDRD Program and the Center for Nonlinear Studies for this work. We thank David Marshall and an anonymous reviewer for their insightful remarks that improved this manuscript.

REFERENCES

Adcroft, A., C. Hill, and J. Marshall, 1997: Representation of topography by shaved cells in a height coordinate ocean model. *Mon. Wea. Rev.*, **125**, 2293–2315, doi:10.1175/1520-0493(1997)125<2293:ROTBSC>2.0.CO;2.

Agra, C., and D. Nof, 1993: Collision and separation of boundary currents. *Deep-Sea Res.*, **40**, 2259–2282, doi:10.1016/0967-0637(93)90103-A.

Amante, C., and B. Eakins, 2009: ETOPO1 1 arc-minute global relief model: Procedures, data sources and analysis. NOAA Tech. Memo. NESDIS NGDC-24, accessed 11 October 2012, doi:10.7289/V5C8276M.

Auer, S., 1987: Five-year climatological survey of the Gulf Stream system and its associated rings. *J. Geophys. Res.*, **92**, 11 709–11 726, doi:10.1029/JC092iC11p11709.

Batchelor, G., 2000: An *Introduction* to Fluid Dynamics. 3rd ed. Cambridge University Press, 658 pp.

Bryan, F. O., M. Hecht, and R. Smith, 2007: Resolution convergence and sensitivity studies with North Atlantic circulation models. Part I: The western boundary current system. *Ocean Modell.*, **16**, 141–159, doi:10.1016/j.ocemod.2006.08.005.

Cane, M., V. Kamenkovitch, and A. Krupitsky, 1998: On the utility and disutility of JEBAR. *J. Phys. Oceanogr.*, **28**, 519–526, doi:10.1175/1520-0485(1998)028<0519:OTUADO>2.0.CO;2.

Charney, J., 1955: The Gulf Stream as an inertial boundary layer. *Proc. Natl. Acad. Sci. USA*, **41**, 731–740, doi:10.1073/pnas.41.10.731.

Chassignet, E., and D. Marshall, 2008: Gulf Stream separation in numerical ocean models. *Ocean Modeling in an Eddying Regime*, Geophys. Monogr., Vol. 177, Amer. Geophys. Union, 39–61.

Dengg, J., 1993: The problem of Gulf Stream separation: A barotropic approach. *J. Phys. Oceanogr.*, **23**, 2182–2200, doi:10.1175/1520-0485(1993)023<2182:TPOGSS>2.0.CO;2.

Deremble, B., N. Wienders, and W. Dewar, 2013: CheapAML: A simple, atmospheric boundary layer model for use in ocean-only model calculations. *Mon. Wea. Rev.*, **141**, 809–821, doi:10.1175/MWR-D-11-00254.1.

Ezer, T., 2016: Revisiting the problem of the Gulf Stream separation: On the representation of topography in ocean models with different types of vertical grids. *Ocean Modell.*, **104**, 15–27, doi:10.1016/j.ocemod.2016.05.008.

——, and G. Mellor, 1992: A numerical study of the variability and separation of the Gulf Stream induced by surface atmospheric forcing and lateral boundary flows. *J. Phys. Oceanogr.*, **22**, 660–682, doi:10.1175/1520-0485(1992)022<0660:ANSOTV>2.0.CO;2.

——, L. Atkinson, W. Corlett, and J. Blanco, 2013: Gulf Stream's induced sea level rise and variability along the U.S. mid-Atlantic coast. *J. Geophys. Res. Oceans*, **118**, 685–697, doi:10.1002/jgrc.20091.

Gawarkiewicz, G. G., R. Todd, A. Plueddemann, M. Andres, and J. Manning, 2012: Direct interaction between the Gulf Stream and the shelfbreak south of New England. *Sci. Rep.*, **2**, 553, doi:10.1038/srep00553.

Gula, J., M. J. Molemaker, and J. McWilliams, 2015: Gulf Stream dynamics along the southeastern U.S. seaboard. *J. Phys. Oceanogr.*, **45**, 690–715, doi:10.1175/JPO-D-14-0154.1.

Haidvogel, D., J. McWilliams, and P. Gent, 1992: Boundary current separation in a quasigeostrophic, eddy-resolving ocean circulation. *J. Phys. Oceanogr.*, **22**, 882–902, doi:10.1175/1520-0485(1992)022<0882:BCSIAQ>2.0.CO;2.

Hogg, N., and H. Stommel, 1985: On the relation between the deep circulation and the Gulf Stream. *Deep-Sea Res.*, **32A**, 1181–1193, doi:10.1016/0198-0149(85)90002-0.

Holland, W., 1972: Baroclinic and topographic influences on the transport in western boundary currents. *Geophys. Fluid Dyn.*, **4**, 187–210, doi:10.1080/03091927208236095.

Hughes, R., 1986: On the role of criticality in coastal flows over irregular bottom topography. *Dyn. Atmos. Oceans*, **10**, 129–147, doi:10.1016/0377-0265(86)90003-5.

Hurlburt, H., and P. Hogan, 2008: The Gulf Stream pathway and the impacts of the eddy-driven abyssal circulation and the deep western boundary current. *Dyn. Atmos. Oceans*, **45**, 71–101, doi:10.1016/j.dynatmoce.2008.06.002.

——, and Coauthors, 2011: Dynamical evaluation of ocean models using the Gulf Stream as an example. *Operational Oceanography in the 21st Century*, A. Schiller and G. B. Brassington, Eds., Springer, 545–609.

Kenwright, D., C. Henze, and C. Levit, 1999: Feature extraction of separation and attachment lines. *IEEE Trans. Visualization Comput. Graphics*, **5**, 135–144, doi:10.1109/2945.773805.

Large, W., J. McWilliams, and S. Doney, 1994: Oceanic vertical mixing: A review and a model with a nonlocal boundary layer parameterization. *Rev. Geophys.*, **32**, 363–403, doi:10.1029/94RG01872.

Lehoucq, R., and D. Sorensen, 1996: Deflation techniques for an implicitly restarted Arnoldi iteration. *SIAM J. Matrix Anal. Appl.*, **17**, 789–821, doi:10.1137/S0895479895281484.

Marshall, D., and C. Tansley, 2001: An implicit formula for boundary current separation. *J. Phys. Oceanogr.*, **31**, 1633–1638, doi:10.1175/1520-0485(2001)031<1633:AIFFBC>2.0.CO;2.

Marshall, J., C. Hill, L. Perelman, and A. Adcroft, 1997: Hydrostatic, quasi-hydrostatic, and non-hydrostatic ocean modelling. *J. Geophys. Res.*, **102**, 5733–5753, doi:10.1029/96JC02776.

Munday, D., and D. Marshall, 2005: On the separation of a barotropic western boundary current from a cape. *J. Phys. Oceanogr.*, **35**, 1726–1743, doi:10.1175/JPO2783.1.

Olson, D. B., G. Podesta, R. Evans, and O. Brown, 1988: Temporal variations in the separation of the Brazil and Malvinas Currents. *Deep-Sea Res.*, **35**, 1971–1990, doi:10.1016/0198-0149(88)90120-3.

Ozgokmen, T., E. Chassignet, and A. Paiva, 1997: Impact of wind forcing, bottom topographs, and inertia on midlatitude jet separation in a quasi-geostrophic model. *J. Phys. Oceanogr.*, **27**, 2460–2476, doi:10.1175/1520-0485(1997)027<2460:IOWFBT>2.0.CO;2.

Parsons, A., 1969: A two-layer model of Gulf Stream separation. *J. Fluid Mech.*, **39**, 511–528, doi:10.1017/S0022112069002308.

Pickart, R., 1994: Interaction of the Gulf Stream and deep western boundary current where they cross. *J. Geophys. Res.*, **99**, 25 155–25 164, doi:10.1029/94JC02217.

——, 1995: Gulf Stream–generated topographic Rossby waves. *J. Phys. Oceanogr.*, **25**, 574–586, doi:10.1175/1520-0485(1995)025<0574:GSTRW>2.0.CO;2.

——, and W. Smethie, 1993: How does the deep western boundary current cross the Gulf Stream? *J. Phys. Oceanogr.*, **23**, 2602–2616, doi:10.1175/1520-0485(1993)023<2602:HDTDWB>2.0.CO;2.

Saba, V., and Coauthors, 2016: Enhanced warming of the northwest Atlantic Ocean under climate change. *J. Geophys. Res.*, **121**, 118–132, doi:10.1002/2015JC011346.

Sarkisyan, A., and V. Ivanov, 1971: Joint effect of baroclinicity and bottom relief as an important factor in the dynamics of sea currents. *USSR Atmos. Oceanic Phys.*, **42**, 173–178.

Schoonover, J., and Coauthors, 2016: North Atlantic barotropic vorticity balances in numerical models. *J. Phys. Oceanogr.*, **46**, 289–303, doi:10.1175/JPO-D-15-0133.1.

Sedberry, G., J. McGovern, and O. Pashuk, 2001: The Charleston Bump: An island of essential fish habitat in the Gulf Stream. *Amer. Fish. Soc. Symp.*, **25**, 3–24.

Shchepetkin, A., and J. McWilliams, 2005: The Regional Ocean Modeling System (ROMS): A split-explicit, free-surface, topography-following-coordinate ocean model. *Ocean Modell.*, **9**, 347–404, doi:10.1016/j.ocemod.2004.08.002.

Spall, M., 1996: Dynamics of the Gulf Stream/deep western boundary current crossover. Part I: Entrainment and recirculation. *J. Phys. Oceanogr.*, **26**, 2152–2168, doi:10.1175/1520-0485(1996)026<2152:DOTGSW>2.0.CO;2.

Stern, M., 1998: Separation of a density current from the bottom of a continental shelf. *J. Phys. Oceanogr.*, **28**, 2040–2049, doi:10.1175/1520-0485(1998)028<2040:SOADCF>2.0.CO;2.

——, and J. Whitehead, 1990: Separation of a boundary jet in a rotating fluid. *J. Fluid Mech.*, **217**, 41–69, doi:10.1017/S0022112090000623.

Tansley, C., and D. Marshall, 2000: On the influence of bottom topography and the deep western boundary current on Gulf Stream separation. *J. Mar. Res.*, **58**, 297–325, doi:10.1357/002224000321511179.

Thompson, J., and W. Schmitz, 1989: A limited-area model of the Gulf Stream: Design, initial experiments, and model-data intercomparison. *J. Phys. Oceanogr.*, **19**, 791–814, doi:10.1175/1520-0485(1989)019<0791:ALAMOT>2.0.CO;2.

Zhang, R., and G. Vallis, 2007: The role of bottom vortex stretching on the path of the North Atlantic western boundary current and on the northern recirculation gyre. *J. Phys. Oceanogr.*, **37**, 2053–2080, doi:10.1175/JPO3102.1.